

## Vibrations of hydrogen and deuterium in solid solution with lutetium

T. J. Udovic and J. J. Rush

*Materials Science and Engineering Laboratory, National Institute of Standards and Technology, Gaithersburg, Maryland 20899*

I. S. Anderson

*Institute Laue-Langevin, 38042 Grenoble Cedex, France*

J. N. Daou\* and P. Vajda†

*Hydrogène dans les Métaux, Centre National de la Recherche Scientifique, Bâtiment 350, Université Paris-Sud, F-91405 Orsay, France*

O. Blaschko

*Institut für Experimentalphysik der Universität Wien, Strudlhofgasse 4, A-1090 Wien, Austria*

(Received 17 November 1993; revised manuscript received 14 April 1994)

The vibrational spectroscopy of hydrogen isotopes in  $\alpha$ -phase solid solution with Lu was probed by incoherent-inelastic-neutron-scattering methods. Low-resolution spectra of H and D located at tetrahedral interstices are qualitatively similar to those of other rare-earth/hydrogen  $\alpha$  phases, indicating a vibrational mode along the  $c$  direction that is  $\sim 30\%$  softer and significantly broader than the doubly degenerate vibrational modes in the basal plane. High-resolution spectra of these broad  $c$ -axis vibrations reveal a temperature- and concentration-dependent line shape believed to consist of local acoustic and optic bands associated with the dynamical coupling of hydrogen atoms paired on either side of a metal atom along the  $c$  direction. Previous diffuse-elastic-neutron-scattering studies indicate the existence of short-range ordering of these hydrogen pairs into  $c$ -axis-oriented chains possessing interchain correlations. The shape and width of these bands at low temperature near the  $\alpha/\beta$ -phase boundary compared to those of the analogous Sc and Y  $\alpha$ -phase systems suggest that the extent of ordering in  $\alpha$ -LuH $_x$  is intermediate with respect to that in the (less ordered)  $\alpha$ -ScH $_x$  and (more ordered)  $\alpha$ -YH $_x$  solid solutions.

### INTRODUCTION

Almost thirty years ago, lutetium was the focus of the earliest work<sup>1</sup> illustrating the unusual stability of rare-earth/hydrogen  $\alpha$ -phase solid solutions. Since that time, a number of other hcp rare-earth metals (e.g., Sc, Y, Tm, Er, and Ho) have been found capable of absorbing varying quantities of hydrogen in  $\alpha$ -phase solid solutions without the formation of long-range-ordered hydride phases, even at low temperatures.<sup>2</sup> The  $\alpha$ -phase hydrogen occupies the tetrahedral interstices of the metal lattice. The stability of the  $\alpha$  phase is believed to result from an unusual short-range pairing order of the hydrogen as revealed by diffuse-elastic-neutron-scattering (DENS) studies.<sup>3</sup> Each  $c$ -axis-aligned pair of H atoms populates adjacent second-nearest-neighbor  $t$  sites, thus straddling a metal atom. These pairs are themselves ordered in chains along the  $c$  direction. The electrical resistivity anomaly occurring between 150 and 170 K in these systems<sup>2</sup> is believed to be evincive of chain formation.<sup>3</sup> Each consecutive hydrogen pair in the chain undergoes a lateral displacement step, giving the chain a zigzag appearance (see Fig. 1). In addition, interchain correlations become significant with increasing H concentration and decreasing temperature, resulting in the possibility of various lateral chain-chain arrangements, also illustrated in Fig. 1.

The details of the concentration- and temperature-

dependent pairing order (i.e., the fraction of paired hydrogen, the distribution of chain lengths, and the extent of lateral interchain correlations) differ among the rare-earth metals.<sup>4</sup> These differences have been manifested by changes in the hydrogen vibrational dynamics characterized via incoherent-inelastic-neutron-scattering (IINS) studies.<sup>5-12</sup> Typically, the  $t$ -site potential in the various

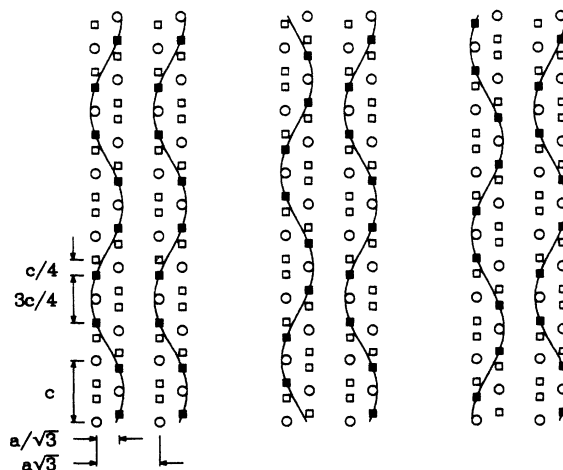


FIG. 1. Schematic of  $c$ -axis-directed chains of hydrogen pairs displaying three possible arrangements of adjacent chains. Circles represent Lu atoms and squares represent  $t$  sites with the closed squares representing H-occupied  $t$  sites.

rare-earth metals has been found to be anisotropic, with the relatively anharmonic H vibrations along the  $c$  direction being 25–30 % lower in energy than the almost harmonic, doubly degenerate H vibrations in the basal plane.

Previous density-of-states measurements<sup>7–10</sup> of the  $c$ -axis vibrations in  $\alpha$ -YH<sub>*x*</sub> and  $\alpha$ -ScH<sub>*x*</sub> have illustrated the sensitivity of the vibrational dynamics to the extent of the hydrogen pairing order. In particular, at high hydrogen concentrations and low temperature, the broad  $c$ -axis vibrational mode was found to be split by  $\sim 4$ –5 meV into local “acoustic” and “optic” bands associated with the dynamic coupling of hydrogen-pair members. It was shown that the splitting could be eliminated by diluting the hydrogen isotopically with deuterium. In effect, the isotopically isolated H atoms were paired only with the heavier D atoms, and dynamic coupling between H and D in the chains was precluded by the differences in mass. Comparison of the width and shape of the  $c$ -axis modes for  $\alpha$ -YH<sub>*x*</sub> and  $\alpha$ -ScH<sub>*x*</sub> highlighted differences in the extent of hydrogen pairing order. The broader and more poorly resolved bands for  $\alpha$ -ScH<sub>*x*</sub> were associated with less extended order of hydrogen pairs, suggestive of shorter chains. Moreover, this less extended order implied that the  $t$ -site potentials in  $\alpha$ -ScH<sub>*x*</sub> possessed a broader distribution of local environments from vicinal H. Because of the shorter interatomic distances in  $\alpha$ -ScH<sub>*x*</sub> compared to  $\alpha$ -YH<sub>*x*</sub>, the perturbations on the  $t$ -site potentials from vicinal H should be more pronounced, further contributing to the broadness of the bands.

Previous vibrational spectra of  $\alpha$ -LuD<sub>0.19</sub> using the 2-T triple-axis spectrometer at Saclay<sup>5</sup> suggested a large ( $\sim 8$  meV) splitting for the  $c$ -axis-polarized D vibration, which was not in line with the results obtained from the analogous  $\alpha$ -phase solutions of hydrogen in Y and Sc using the BT-4 Be-filter spectrometer at NIST.<sup>7–10</sup> It was our intention to investigate this possible discrepancy. Hence, to make a more thorough comparison of hydrogen dynamics in the different rare-earth metals under identical experimental conditions, a study was undertaken of hydrogen and deuterium dissolved in Lu.

#### EXPERIMENTAL DETAILS

Two polycrystalline, rectangular Lu plates (99.99+ % purity,  $50 \times 30 \times 1$  mm<sup>3</sup>, 16 g each) were obtained from the Ames Laboratory Materials Preparation Center at Iowa State University. The thin-plate geometry was necessitated by the significant neutron-absorption cross section for Lu. The plates were initially annealed at 973 K in vacuum ( $< 2 \times 10^{-8}$  torr) for 24 h. One plate was kept as a blank and was subjected to the same thermal treatments as the other H (D)-loaded plate. Hydrogen and deuterium charging of the other plate was accomplished via gas-phase absorption at 873–923 K using a calibrated volume. Over the course of the measurements, this plate was charged four different times to yield  $\alpha$ -LuH<sub>*x*</sub> ( $x=0.19$  and 0.06) and  $\alpha$ -LuD<sub>*x*</sub> ( $x=0.19$  and 0.09). Gravimetric measurements of all targeted H and D concentrations were in good agreement. After charging, the sample was sealed under He in an Al cell and mounted in a cryostat or displax for temperature regula-

tion. Between charges, IINS measurements were performed, followed by evacuation of the H or D at 1223 K in preparation for the next concentration.

All results were obtained at the Neutron Beam Split-Core Reactor (NBSR) at NIST with the BT-4 spectrometer using the Cu(220) monochromator with pre- and post-collimations of 20' or 40' in combination with either a Be-filter (low-resolution) or Be-graphite-Be-filter (high-resolution) analyzer, depending on the desired instrumental resolution. The particular resolution (full width at half maximum, FWHM) used in each case is indicated in the figures by the horizontal bars beneath the spectral peaks. Due to the high absorption cross section, scattering measurements were taken in reflection with a 115° scattering angle.

#### RESULTS AND DISCUSSION

Initial measurements of the Lu blank indicated a flat featureless spectrum over the range of energies covered in this study. This rendered unnecessary the subtraction of the Lu blank spectrum from the hydride spectra. Figure 2 displays low-resolution spectra for  $\alpha$ -LuH<sub>*x*</sub> at 4 K portraying the twin-peak structure due to the lower-energy  $c$ -axis mode and the higher-energy basal-plane modes. The three upper spectra of  $\alpha$ -LuH<sub>0.19</sub> (which possesses a hydrogen concentration very close to the  $\alpha$ -LuH<sub>*x*</sub>/ $\beta$ -LuH<sub>2</sub> phase boundary) represent different sample orientations  $\xi$ , defined as the angle between the neutron-beam axis and the surface-normal vector of the sample. Clearly, the relative scattering intensities of the normal-mode vibrations are dependent on  $\xi$ , indicating that the poly-

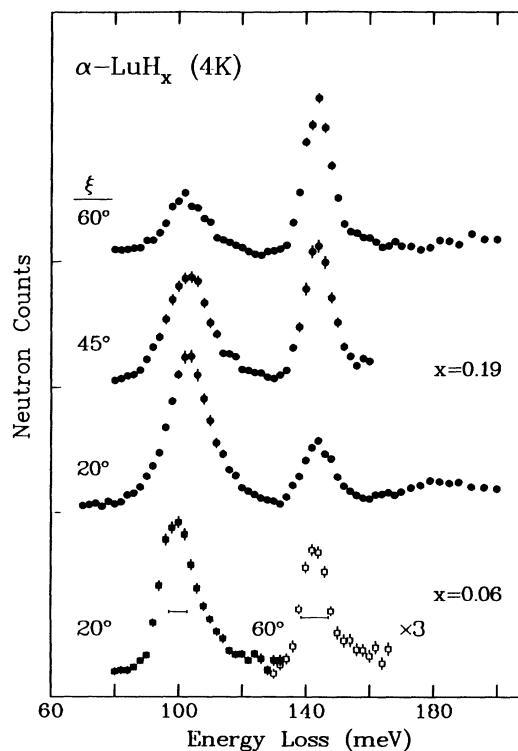


FIG. 2. Low-resolution IINS spectra of  $\alpha$ -LuH<sub>*x*</sub> at 4 K. The angle  $\xi$  is defined in the text.

crystalline samples possessed some texture, with a tendency for the basal planes of the microcrystals to be approximately parallel to the sample surface plane, as seen previously for polycrystalline Sc.<sup>10</sup> Thus, scattering intensities for the vibrational features were maximized in the rest of this study by adjusting  $\xi$  to  $20^\circ$  for measurements of the  $c$ -axis mode and to  $60^\circ$  for measurements of the basal-plane modes.

Gaussian fits of the spectral features in Fig. 2 were performed, including a multiphonon sideband at  $\sim 12$  meV higher energy due to low-energy Lu lattice modes. The position of this sideband is consistent with phonon-dispersion-curve data reported for  $\alpha$ -LuD<sub>x</sub>.<sup>5</sup> In  $\alpha$ -ScH<sub>x</sub>,<sup>9</sup> the multiphonon sideband was situated  $\sim 20$  meV above the main peaks and was a larger fraction of the overall intensity. The smaller displacement and intensity of the sideband in  $\alpha$ -LuH<sub>x</sub> is to be expected due to the fourfold larger atomic mass of Lu compared to Sc. The fits of the H vibrational spectra for  $\alpha$ -LuH<sub>0.19</sub> establish the  $c$ -axis and basal-plane mode energies at 102.8 and 143.5 meV, respectively. The weak  $c$ -axis overtone (evident in the spectrum for  $\xi=20^\circ$ ) at  $\sim 182$  meV results in a ratio of  $\sim 1.78$  for the second- to first-excited-state energies of the  $c$ -axis vibration. Similar analysis of the  $\alpha$ -LuH<sub>0.06</sub> spectrum yields  $c$ -axis and basal-plane mode energies of 98.3 and 142.7 meV, respectively. Again, these spectra verify the anisotropy and anharmonicity of the rare-earth  $t$ -site potential along the  $c$  axis.

Figure 3 shows the low-resolution IINS spectra of  $\alpha$ -LuD<sub>x</sub> at 4 K. The Gaussian fits of the spectral features establish the  $c$ -axis and basal-plane mode energies at 76.2

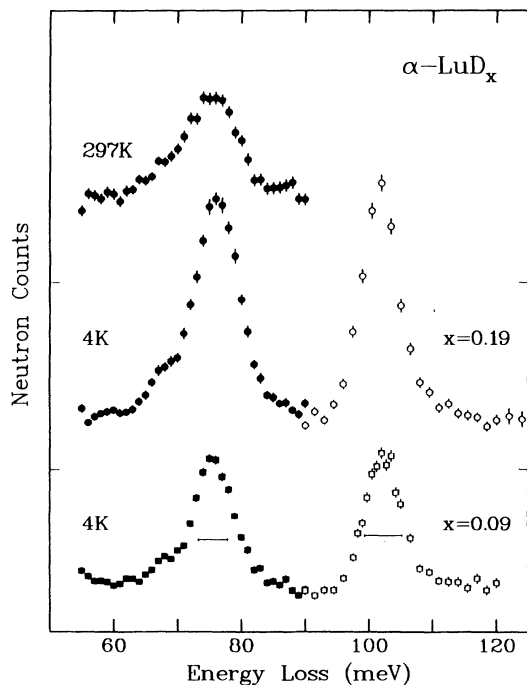


FIG. 3. Low-resolution IINS spectra of  $\alpha$ -LuD<sub>x</sub> at 4 K. Upper spectrum refers to the  $c$ -axis mode for  $\alpha$ -LuD<sub>0.19</sub> at 297 K. Closed symbols represent  $\xi=20^\circ$ , open symbols represent  $\xi=60^\circ$ . The angle  $\xi$  is defined in the text.

and 101.7 meV, respectively, for  $\alpha$ -LuD<sub>0.19</sub> and 75.7 and 102.2 meV, respectively, for  $\alpha$ -LuD<sub>0.09</sub>. The low-energy shoulder at  $\sim 68$  meV for both concentrations is close in energy to that reported previously for  $\alpha$ -LuD<sub>0.19</sub>.<sup>5</sup> However, this shoulder is found to be a minor component of the  $c$ -axis mode band and does not change significantly with concentration or temperature (see the upper spectrum in Fig. 3).

Table I summarizes the spectral parameters obtained from Figs. 2 and 3 and compares them to other investigated  $\alpha$ -phase systems. After correction for the instrumental resolution, it is evident that the  $c$ -axis vibrations are intrinsically much broader than the basal-plane vibrations, similar to the previously investigated  $\alpha$ -phase systems. Again, we believe that this broadness is a reflection of the pairing order that is known to occur along the  $c$  axis. Nonetheless, the relatively sharp basal-plane mode does broaden somewhat as the H (D) concentration increases, as seen for  $\alpha$ -ScH<sub>x</sub>,<sup>10</sup> indicative of more significant interchain (i.e., lateral H-H) interactions at the higher concentrations.

The  $c$ -axis line shape was better resolved under high-resolution conditions, as is shown by the low-temperature spectra in Figs. 4 and 5. In Fig. 4, the high-concentration spectrum of  $\alpha$ -LuH<sub>0.19</sub> displays a complex line shape consistent with the presence of two poorly resolved bands at  $\sim 101$  and 105 meV which we assign to the lower-energy "acoustic" and higher-energy "optic" bands of the dynamically coupled hydrogen pairs. Lowering the concentration to  $\alpha$ -LuH<sub>0.06</sub> yields the bottom spectrum. The entire band is shifted several meV lower in energy. The acoustic component is still relatively sharp (at  $\sim 98$  meV), whereas the optic component is now smeared out. This is in excellent agreement with the concentration-dependent

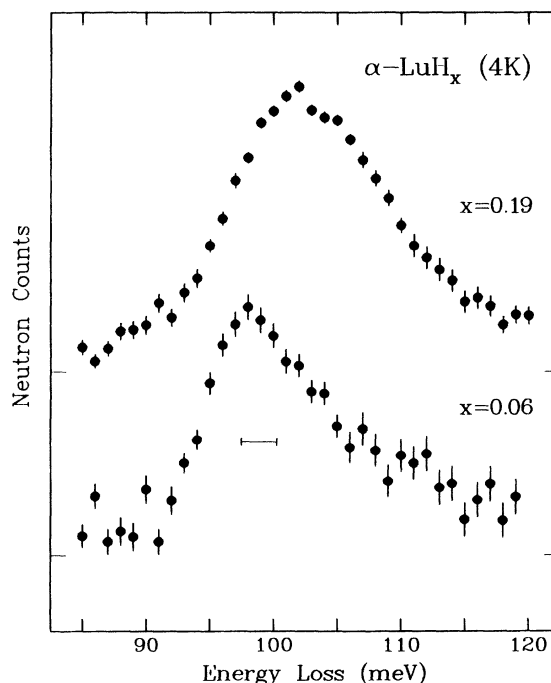


FIG. 4. High-resolution IINS spectra of the  $c$ -axis mode for  $\alpha$ -LuH<sub>x</sub> at 4 K.

TABLE I. Comparison of rare-earth/hydrogen (and deuterium)  $\alpha$  phases below 10 K. The entries refer to data taken under the low-resolution configuration analyzed by Gaussian fits. Note that all fitting errors (in parentheses) are in the last digit given.

	Normal-mode energies			Measured <sup>a</sup> /intrinsic linewidths (meV FWHM)		Lattice parameters <sup>b</sup>	
	( <i>c</i> axis)	( <i>ab</i> plane)	$E_c/E_{ab}$	( <i>c</i> axis)	( <i>ab</i> plane)	<i>a</i> (nm)	<i>c</i> (nm)
	$E_c$ (meV)	$E_{ab}$ (meV)		$\Delta E_m/\Delta E_i$	$\Delta E_m/\Delta E_i$		
$\alpha$ -ScH <sub>0.34</sub> <sup>c</sup>	103.5(3)	1.47.5(1)	0.702	16.9/15.7	10.1/4.4	0.3366	0.5297
$\alpha$ -ScD <sub>0.34</sub> <sup>d</sup>	79.0(1)	107.3(1)	0.736	10.0/8.6	7.5/3.9	0.3338	0.5299
$\alpha$ -YH <sub>0.18</sub> <sup>e</sup>	100.1(2)	134.2(5)	0.746	11.3/9.6	8.7/3.1	0.3664	0.5790
$\alpha$ -YD <sub>0.18</sub> <sup>e</sup>	75.8(1)	96.3(1)	0.787	8.5/6.9	6.1/1.8	0.3662	0.5778
$\alpha$ -LuH <sub>0.06</sub>	98.3(1)	142.7(1)	0.689	13.0/11.6	9.3/3.1	0.3511	0.5568
$\alpha$ -LuH <sub>0.19</sub>	102.8(3)	143.5(1)	0.716	16.2/15.0	9.8/4.3	0.3525	0.5608
$\alpha$ -LuD <sub>0.09</sub>	75.7(1)	102.2(1)	0.741	7.9/6.2	6.9/3.2	0.3513	0.5575
$\alpha$ -LuD <sub>0.19</sub>	76.2(1)	101.7(1)	0.749	8.9/7.4	7.3/4.0	0.3522	0.5604

<sup>a</sup>Measured linewidths are estimated by fitting the entire band (including any asymmetries) with a single Gaussian for comparison with other rare-earth data. Calculated intrinsic linewidths [ $\Delta E_i^2 = (\Delta E_m^2 - \Delta E_r^2)$ ] are based on the most recent determination of the BT-4 instrumental resolution  $\Delta E_r$  under the low-resolution configuration.

<sup>b</sup>Reference 13.

<sup>c</sup>Reference 10.

<sup>d</sup>Reference 14.

<sup>e</sup>Reference 7.

behavior observed for  $\alpha$ -YH<sub>x</sub>.<sup>8</sup> The downward shift in the entire band has been attributed to the relaxation of coherent strain ordering along the *c* direction as the H concentration decreases, which leads to a larger average metal-hydrogen separation. The persistence of the acoustic band at the different concentrations illustrates its relative insensitivity to the details of the hydrogen-pair order, being chiefly dependent on the metal-hydrogen interac-

tion. In contrast, the variations in sharpness and intensity of the optic band with H concentration correlate with variations in the extent of the hydrogen-pair order, since this band is dependent on both metal-hydrogen and hydrogen-hydrogen interactions. At high H concentrations, coherency strains produce highly correlated pair configurations (i.e., a high degree of short-range order), which results in a relatively sharp, well-defined optic band. The diffuseness of the band at lower H concentrations is a manifestation of relatively less short-range order. In this case, there are more unpaired H atoms, and the remaining paired H atoms likely reside in shorter chains possessing a distribution of chain lengths. Hence, the H atoms, on average, experience a broader array of local environments, and therefore a broader distribution of H-H interactions.

The concentration-dependent behavior of the *c*-axis band for  $\alpha$ -LuD<sub>x</sub> in Fig. 5 is consistent with that of  $\alpha$ -LuH<sub>x</sub>. For  $\alpha$ -LuD<sub>0.19</sub>, the highest-resolution line shape (shown by the top spectrum) is flat topped, suggestive of the presence of both the acoustic and optic components at  $\sim 74$  and  $77$  meV in an unresolved doublet. Lowering the concentration to  $\alpha$ -LuD<sub>0.09</sub> results in a narrowing and downshifting of the overall band. This is consistent with the expected dissipation of the optic band which accompanies a decrease in the short-range order.

Comparison of the low-temperature  $\alpha$ -LuD<sub>0.19</sub> spectrum in Fig. 5 with the previous triple-axis measurement<sup>5</sup> indicates that they are in good agreement. Moreover, even though the room-temperature triple-axis spectrum has been tentatively described by a three-peak structure,<sup>5</sup> the actual data, within statistics, are not inconsistent with the corresponding room-temperature Be-filter spectrum in Fig. 3. Possessing a better signal-to-noise ratio, the Be-filter spectrum suggests that the room-temperature line shape is, in reality, less complex. Thus, the apparent

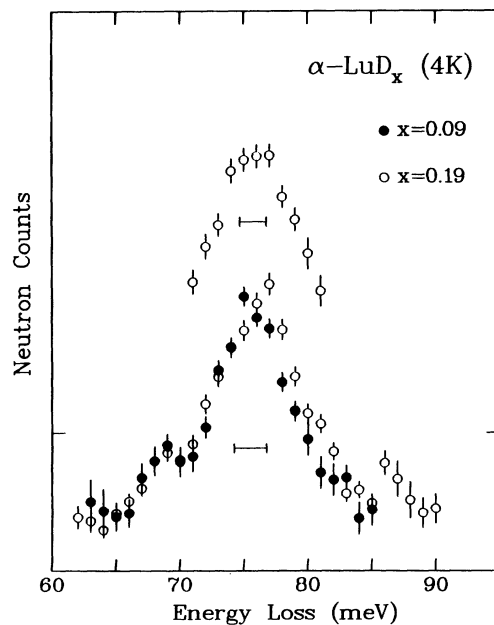


FIG. 5. High-resolution IINS spectra of the *c*-axis mode for  $\alpha$ -LuD<sub>x</sub> at 4 K. Upper spectrum refers to  $\alpha$ -LuD<sub>0.19</sub> at 25% better resolution and corresponds with the shifted baseline designated by the horizontal tick marks.

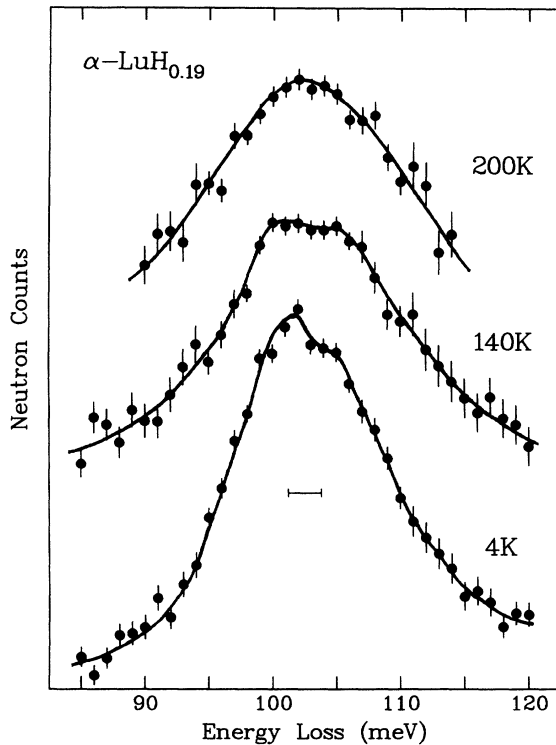


FIG. 6. High-resolution IINS spectra of the  $c$ -axis mode for  $\alpha$ -LuH<sub>0.19</sub> as a function of temperature. Lines are drawn only as guides to the eye.

disagreement between the triple-axis and Be-filter results is likely not due to differences in the data, but rather to differences in interpretation. In Fig. 5, the 68-meV shoulder is clearly resolved at both concentrations measured. However, since it is only a minor component of the overall intensity, it appears to be unrelated to the major band splitting. In the previous triple-axis study, this shoulder and the unresolved major band at higher energy were mistaken for the acoustic and optic components of a  $c$ -axis doublet, leading to the assignment of the larger-than-expected 8-meV splitting. The true origin of the 68-meV shoulder remains puzzling at present. One might consider it a vibrational contribution from the D atoms at the end of the chains, but this does not agree with the observed energy or the insensitivity to concentration changes. Furthermore, since the spectra were collected at 4 K, there is no possibility that it is due to multiphonon scattering at this energy. The purity of the metal and gases used and the lack of a comparable feature in the  $\alpha$ -LuH<sub>x</sub> spectra are arguments against it being a contribution from D atoms trapped at impurity sites. In short, after considering various possibilities, we have been unable to find a satisfactory model which can account for the concentration and temperature dependence of the measured spectra.

Figure 6 shows high-resolution IINS spectra of the  $c$ -axis vibration in  $\alpha$ -LuH<sub>0.19</sub> as a function of temperature.

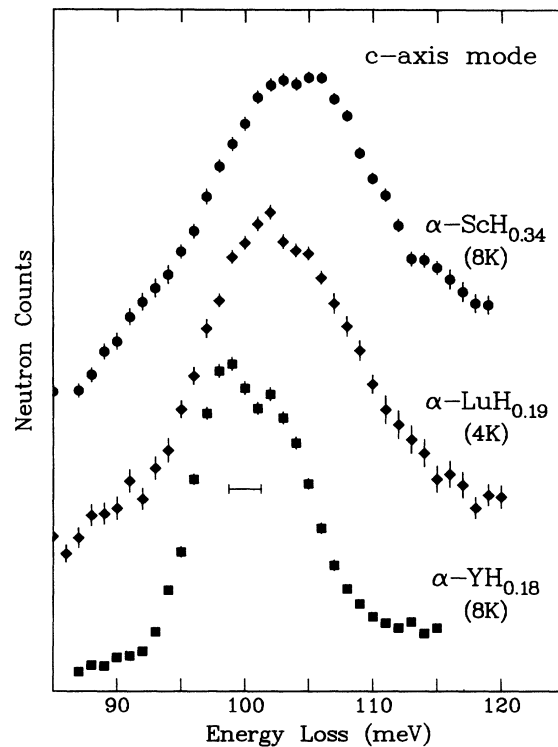


FIG. 7. A comparison of high-resolution IINS spectra below 10 K of the  $c$ -axis mode for Y, Lu, and Sc high-H-concentration  $\alpha$ -phases.

As the temperature is increased from 4 to 200 K, the  $c$ -axis-mode splitting disappears, which indicates increased H disorder within the metal lattice. This is in accord with the temperature-dependent behavior found for  $\alpha$ -YH<sub>0.18</sub>.<sup>8</sup>

Finally, it is interesting to compare the  $c$ -axis vibrational line shapes of the hydrogen-rare-earth systems measured thus far. Figure 7 displays the low-temperature  $c$ -axis spectra for the three investigated high-concentration H/rare-earth  $\alpha$  phases in the order of decreasing lattice constant  $c$  from Y (0.579 nm) to Lu (0.561 nm) to Sc (0.530 nm). Proceeding from Y to Sc, the overall line shape becomes broader and the splitting becomes less distinct. This is clearly suggestive of decreasing H-pair order as the lattice constant  $c$  decreases as mentioned earlier, with  $\alpha$ -LuH<sub>x</sub> exhibiting an intermediate degree of short-range order, somewhat less ordered than  $\alpha$ -YH<sub>x</sub> and somewhat more ordered than  $\alpha$ -ScH<sub>x</sub>. Of course the present measurements cannot define the admixture of intrachain and interchain interactions which controls the details of the hydrogen dynamics. Further diffraction and diffuse-scattering experiments are required to better reveal the details of H (D) ordering in these hydrogen-rare-earth systems as a function of hydrogen concentration. Extension to other rare earths which exhibit a much more limited  $\alpha$ -phase region (e.g., Tm, Er, and Ho) would also be desirable.

\*Deceased.

†Also at Laboratoire des Solides Irradiés, Ecole Polytechnique, F-91128 Palaiseau, France.

- <sup>1</sup>J. N. Daou and J. Bonnet, C. R. Acad. Sci. Paris **261**, 1675 (1965).
- <sup>2</sup>J. N. Daou and P. Vajda, Ann. Chim. (Paris) **13**, 567 (1988).
- <sup>3</sup>O. Blaschko, G. Krexner, J. N. Daou, and P. Vajda, Phys. Rev. Lett. **55**, 2876 (1985).
- <sup>4</sup>O. Blaschko, J. Less-Common Met. **172-174**, 237 (1991).
- <sup>5</sup>O. Blaschko, G. Krexner, L. Pintschovius, P. Vajda, and J. N. Daou, Phys. Rev. B **38**, 9612 (1988).
- <sup>6</sup>O. Blaschko, J. Pleschiutchnig, L. Pintschovius, J. P. Burger, J. N. Daou, and P. Vajda, Phys. Rev. B **40**, 907 (1989).
- <sup>7</sup>I. S. Anderson, J. J. Rush, T. Udovic, and J. M. Rowe, Phys. Rev. Lett. **57**, 2822 (1986).
- <sup>8</sup>I. S. Anderson, N. F. Berk, J. J. Rush, and T. J. Udovic, Phys. Rev. B **37**, 4358 (1988).
- <sup>9</sup>T. J. Udovic, J. J. Rush, I. S. Anderson, and R. G. Barnes, Phys. Rev. B **41**, 3460 (1990).
- <sup>10</sup>T. J. Udovic, J. J. Rush, N. F. Berk, and I. S. Anderson, Phys. Rev. B **45**, 12 573 (1992).
- <sup>11</sup>S. M. Bennington, D. K. Ross, M. J. Benham, A. D. Taylor, Z. A. Bowden, and R. Osborn, Phys. Lett. A **151**, 325 (1990).
- <sup>12</sup>S. M. Bennington, R. Osborn, D. K. Ross, and M. J. Benham, J. Less-Common Met. **172-174**, 440 (1991).
- <sup>13</sup>P. Vajda and J. N. Daou, in *Hydrogen-Metal Systems*, edited by A. Aladjem and F. A. Lewis (VCH, Weinheim, in press), Vol. 1, Chap. 3a.
- <sup>14</sup>T. J. Udovic, J. J. Rush, N. F. Berk, and I. S. Anderson (unpublished).